Dynamic Stress Intensity Factors around Two Cylindrical Cracks in an Infinite Elastic Medium Subject to Impact Load

Shouetsu Itou

Department of Mechanical Engineering, Kanagawa University
Rokkakubashi, Kanagawa-ku, Yokohama 221-8686, Japan
itous001@kanagawa-u.ac.jp

Abstract

Dynamic stresses are solved for two cylindrical cracks in an infinite elastic medium. Incident shock stress waves pass through the elastic medium normal to the cracks' axis. In the Laplace transform domain, the mixed boundary value equations with respect to stresses and displacements are reduced to two sets of dual integral equations by means of the Fourier transform technique. To solve these equations, the differences in the cracks' surface displacements are expanded in a series of functions that are zero outside the cracks. The boundary conditions inside the cracks are satisfied by means of the Schmidt method. Stress intensity factors are defined in the Laplace transform domain and are numerically inverted in physical space. Numerical calculations are performed for the dynamic stress intensity factors corresponding to some typical shapes assumed for the cylindrical cracks.

Keywords: Stress intensity factor, Two cylindrical cracks, Transient stresses, Numerical Laplace inversion, Schmidt method

1 Introduction

Structural components are usually weakened during their lifetime by cracks initiated by fatigue or corrosion. Initial cracks are characterized by their small size and planar surfaces. If mixed mode loading is applied to the cracked material, however, the crack will not propagate in a plane, but may curve to form a

shell-shaped crack. For non-planar cracks of this type, analytical methods cannot be used to solve for the stress intensity factors. In these cases, solution of the stress intensity factors requires the use of numerical techniques such as the finite element method, the surface integral method, etc.

If a numerical method is utilized to solve the stress intensity factors for a shell-shaped crack, the accuracy of the results must be verified. For this purpose, it is useful to compare the results with results from the analytical method for a crack of similar shape to the shell-shaped crack. In a previous study [2], the author solved the transient stresses around a cylindrical crack in an infinite elastic medium during the passage of incident stress waves. Since the results for the cylindrical crack obtained using the numerical method were coincident with the analytical solutions given in Ref. [2] with acceptable accuracy, the numerical method can also be used to solve the stress intensity factors for a shell-shaped crack.

For a similar purpose, the transient stresses around two cylindrical cracks in an infinite medium are also solved using an analytical method in this study. The incident shock stress waves impinge normal to the cracks' axis. In the Laplace domain, differences in the displacements at the cracks' surfaces are expanded in a series of functions that diminish to zero outside the cracks. The unknown coefficients in the series are solved so as to satisfy the stress-free conditions inside the cracks with the Schmidt method [2, 4]. The stress intensity factors are defined in the Laplace domain, and they are inverted numerically in physical space using Miller and Guy's method [3].

2   Stress intensity factors for two shell-shaped cracks

Consider an infinite elastic medium weakened by two non-planar cracks similar to the shell-shaped cracks shown in Fig. 1. The stress intensity factors for these cracks can only be solved with a numerical method such as the finite element method, the surface integral method, etc. It is therefore necessary to verify
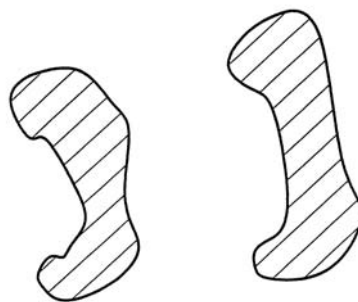

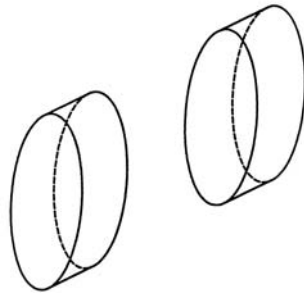Figure 1 Two shell-shaped cracks in an infinite elastic medium.

Figure 2 Two cylindrical cracks in an infinite elastic medium.

whether the accuracy of the numerical results is satisfactory or not. If the same numerical method is utilized to solve the stress intensity factors for two cylindrical cracks as shown in Fig. 2, it can be verified whether the numerical results given by the numerical method are reliable or not by comparing the results with those obtained by the analytical method.

3 Fundamental Equations

With respect to the cylindrical coordinates (r, θ, z), consider two cylindrical cracks located on $r = b$ and extending from $z = -f$ to $z = -e$ and from $z = e$ to $z = f$, as shown in Fig. 3. For the sake of convenience, the infinite medium is divided into a cylinder (1) denoted by $(0 \leq r \leq b)$, and an infinite region (2) denoted by $(b \leq r)$.
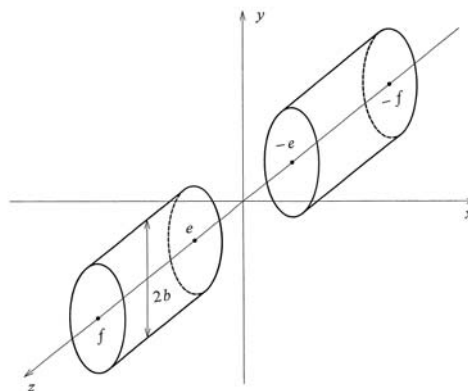

Figure 3 Two cylindrical cracks and coordinate system.

The rectangular coordinates (x, y, z) are used in the expression of the incident stress waves; these are related to the cylindrical coordinates (r, θ, z) by the equations:

$$x = r\cos(\theta), \qquad y = r\sin(\theta), \quad z = z \,. \tag{1}$$

Consequently, the incident stress waves that impinge on the cracks as shown in Fig. 4 are expressed by the equations:

$$\tau_{xx}^{(i)} = p\,H[t + (x-b)/c_L], \quad \tau_{yy}^{(i)} = \tau_{zz}^{(i)} = \tau_{yx}^{(i)} = \tau_{yz}^{(i)} = 0 \tag{2}$$

where p is a constant, c_L is the longitudinal wave velocity, $H(t)$ is the Heaviside unit step function and time, t, is zero when the wave front reaches the crack surface $(r = b, \quad \theta = 0)$.
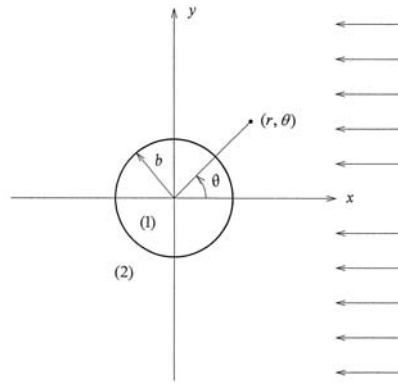

Figure 4 Incident stress waves expressed by rectangular coordinates $(x, \ y, \ z)$.

The incident waves can be defined in the cylindrical coordinate system (r, θ, z) by the equation:

$$\tau_{rr}^{(i)} = pH[t + (x-b)/c_L]\cos^2\theta, \qquad \tau_{\theta\theta}^{(i)} = pH[t + (x-b)/c_L]\sin^2\theta,$$
$$\tau_{r\theta}^{(i)} = -(1/2)\times pH[t + (x-b)/c_L]\sin(2\theta), \qquad \tau_{zz}^{(i)} = \tau_{rz}^{(i)} = \tau_{\theta z}^{(i)} = 0 \tag{3}$$

Thus, the boundary conditions for the scattered field are given by the equations:

$$\tau_{rr1} = \tau_{rr2}, \quad \tau_{rz1} = \tau_{rz2}, \quad \tau_{r\theta1} = \tau_{r\theta2}, \qquad \text{at} \quad r = b, \ \ |z| \le \infty \tag{4}$$

$$\tau_{rr1} = -\tau_{rr}^{(i)}, \quad \tau_{rz1} = -\tau_{rz}^{(i)}, \quad \tau_{r\theta1} = -\tau_{r\theta}^{(i)}, \quad \text{at} \quad r = b, \ \ e < |z| \le f \tag{5}$$

$$u_{r1} = u_{r2}, \quad u_{z1} = u_{z2}, \quad u_{\theta1} = u_{\theta2} \quad \text{at} \quad r = b, \ \ 0 \le |z| < e, \ \ f < |z| \tag{6}$$

where u_r, u_θ and u_z are defined as the r, θ and z displacement components, respectively, and subscripts 1 and 2 denote the variables for the cylinder (1) and the infinite region (2), respectively.

Using the cylindrical coordinate system (r, θ, z), displacement potential functions ϕ_n, φ_n and χ_n are introduced according to the following relationships [5],

$$u_r = \sum_{n=0}^{\infty} [\partial \phi_n / \partial r - \partial^2 \varphi_n / (\partial r \partial z) + (n/r) \times \chi_n] \cos(n\theta),$$

$$u_\theta = \sum_{n=0}^{\infty} [-(n/r) \times \phi_n + (n/r) \times \partial \varphi_n / \partial z - \partial \chi_n / \partial r] \sin(n\theta), \qquad (7)$$

$$u_z = \sum_{n=0}^{\infty} [\partial \phi_n / \partial z + \partial^2 \varphi_n / \partial r^2 + (1/r) \times \partial \varphi_n / \partial r - (n/r)^2 \times \varphi_n] \cos(n\theta).$$

Substituting Eq. (7) into the equations of motion yields:

$$\partial^2 \phi_n / \partial r^2 + (1/r) \times \partial \phi_n / \partial r - (n/r)^2 \times \phi_n + \partial^2 \phi_n / \partial z^2 = 1/c_L^2 \times \partial^2 \phi_n / \partial t^2,$$

$$\partial^2 \varphi_n / \partial r^2 + (1/r) \times \partial \varphi_n / \partial r - (n/r)^2 \times \varphi_n + \partial^2 \varphi_n / \partial z^2 = 1/c_T^2 \times \partial^2 \varphi_n / \partial t^2, \qquad (8)$$

$$\partial^2 \chi_n / \partial r^2 + (1/r) \times \partial \chi_n / \partial r - (n/r)^2 \times \chi_n + \partial^2 \chi_n / \partial z^2 = 1/c_T^2 \times \partial^2 \chi_n / \partial t^2,$$

with

$$c_L^2 = (\lambda + 2\mu)/\rho, \qquad c_T^2 = \mu/\rho. \qquad (9)$$

In Eqs. (8) and (9), c_T is the transverse elastic wave velocity; λ and μ are Lame's elastic constants and ρ is the density of the material.

The stresses in the medium are expressed in terms of ϕ_n, φ_n and χ_n by the equations:

$$\tau_{rr} = \sum_{n=0}^{\infty} \{(\lambda/c_L^2) \times \partial^2 \phi_n / \partial t^2 + 2\mu [\partial^2 \phi_n / \partial r^2 - \partial^3 \varphi_n / \partial r^2 \partial z + (n/r) \times \partial \chi_n / \partial r$$
$$- (n/r^2) \times \chi_n]\} \cos(n\theta)$$

$$\tau_{\theta\theta} = \sum_{n=0}^{\infty} \{(\lambda/c_L^2) \times \partial^2 \phi_n / \partial t^2 + (2\mu/r) \times [\partial \phi_n / \partial r - (n^2/r) \times \phi_n$$
$$+ (n^2/r) \times \partial \varphi_n / \partial z - \partial^2 \varphi_n / \partial r \partial z + (n/r) \times \chi_n - n\chi_n]\} \cos(n\theta)$$

$$\tau_{zz} = \sum_{n=0}^{\infty} \{(\lambda/c_L^2) \times \partial^2 \phi_n / \partial t^2 + 2\mu [\partial^2 \phi_n / \partial z^2 - (n/r)^2 \times \partial \varphi_n / \partial z$$
$$+ (1/r) \times \partial^2 \varphi_n / \partial r \partial z + \partial^3 \varphi_n / \partial r^2 \partial z]\} \cos(n\theta)$$

$$\tau_{rz} = \sum_{n=0}^{\infty} \mu \{2 \partial^2 \phi_n / \partial r \partial z + \partial^3 \varphi_n / \partial r^3 + (1/r) \times \partial^2 \varphi_n / \partial r^2 - [(n^2+1)/r^2] \times \partial \varphi_n / \partial r$$
$$+ (2n^2/r^3) \times \varphi_n - \partial^3 \varphi_n / \partial r \partial z^2 + (n/r) \times \partial \chi_n / \partial z\} \cos(n\theta)$$

$$\tau_{r\theta} = \sum_{n=0}^{\infty} \mu \{(2n/r) \times (\phi_n/r - \partial \phi_n / \partial r) + (2n/r) \times \partial^2 \varphi_n / \partial r \partial z - (2n/r^2) \times \partial \varphi_n / \partial z$$
$$+ (1/r) \times \partial \chi_n / \partial r - (n/r)^2 \times \chi_n - \partial^2 \chi_n / \partial r^2\} \sin(n\theta)$$

$$\tau_{\theta z} = \sum_{n=0}^{\infty} \mu \{-(2n/r) \times \partial \phi_n / \partial z + (n/r) \times [(n/r)^2 \times \varphi_n + \partial^2 \varphi_n / \partial z^2$$
$$- (1/r) \times \partial \varphi_n / \partial r - \partial^2 \varphi_n / \partial r^2] - \partial^2 \chi_n / \partial r \partial z\} \sin(n\theta)$$

$$(10)$$

4 Analysis

To obtain the solution, we introduce the Laplace transforms,

$$g*(s) = \int_0^\infty g(t) \exp(-st)\, dt, \qquad g(t) = 1/(2\pi i) \int_{Br.} g*(s) \exp(st)\, ds \tag{11}$$

and the Fourier transforms,

$$\bar{f}(\xi) = \int_{-\infty}^\infty f(z) \exp(i\xi z)\, dz, \quad f(z) = 1/(2\pi i) \times \int_{-\infty}^\infty \bar{f}(\xi) \exp(-i\xi z)\, d\xi. \tag{12}$$

Applying Eqs. (11) and (12) to Eq. (8) yields:

$$[d^2/dr^2 + (1/r)d/dr - (n^2/r^2 + \xi^2 + s^2/c_L^2)]\, \bar{\phi}_n* = 0,$$

$$[d^2/dr^2 + (1/r)d/dr - (n^2/r^2 + \xi^2 + s^2/c_T^2)]\, \bar{\varphi}_n* = 0, \tag{13}$$

$$[d^2/dr^2 + (1/r)d/dr - (n^2/r^2 + \xi^2 + s^2/c_T^2)]\, \bar{\chi}_n* = 0.$$

The solutions of Eq. (13) for the cylinder (1) and the infinite region (2) assume the following forms:

$$\bar{\phi}_{n1}* = A_n^{(1)}(\xi)\, I_n(\alpha r), \quad \bar{\varphi}_{n1}* = i\, B_n^{(1)}(\xi)\, I_n(\beta r), \quad \bar{\chi}_{n1}* = C_n^{(1)}(\xi)\, I_n(\beta r) \tag{14}$$

$$\bar{\phi}_{n2}* = A_n^{(2)}(\xi)\, K_n(\alpha r), \quad \bar{\varphi}_{n2}* = i\, B_n^{(2)}(\xi)\, K_n(\beta r), \quad \bar{\chi}_{n2}* = C_n^{(2)}(\xi)\, K_n(\beta r) \tag{15}$$

with

$$\alpha = (\xi^2 + s^2/c_L^2)^{1/2}, \qquad \beta = (\xi^2 + s^2/c_T^2)^{1/2} \tag{16}$$

where $K_n(\xi)$ and $I_n(\xi)$ are modified Bessel functions, and the unknown coefficients $A_n^{(2)}(\xi)$, $B_n^{(2)}(\xi)$, $C_n^{(2)}(\xi)$ can be expressed with the unknown coefficients $A_n^{(1)}(\xi)$, $B_n^{(1)}(\xi)$, $C_n^{(1)}(\xi)$ by employing Eq. (4) as shown in Ref. [2].

In order to satisfy Eq. (6), the differences in the displacements at $r = b$ in the Laplace domain are expanded by means of the following series:

$$\pi(u_{r1b}* - u_{r2b}*) = \sum_{n=0}^\infty \{\sum_{m=1}^\infty a_{mn} \frac{1}{2m} \sin[m \sin^{-1}\{(e+f-2|z|)/(f-e)\} - m\pi/2]\} \cos(n\theta)$$

$$\text{for} \quad e < |z| < f$$

$$= 0 \qquad\qquad \text{for} \quad 0 \le |z| < e, \quad f < |z| < \infty \tag{17}$$

$$\pi(u_{\theta1b}* - u_{\theta2b}*) = \sum_{n=0}^\infty \{\sum_{m=1}^\infty b_{mn} \frac{1}{2m} \sin[m \sin^{-1}\{(e+f-2|z|)/(f-e)\} - m\pi/2]\} \sin(n\theta)$$

$$\text{for} \quad e < |z| < f$$

$$= 0 \qquad\qquad \text{for} \quad 0 \le |z| < e, \quad f < |z| < \infty \tag{18}$$

$$\pi\,(u_{z1b}* - u_{z2b}*) = \sum_{n=0}^{\infty}\{\sum_{m=1}^{\infty} c_{mn} \frac{1}{2m}\sin[m\,\sin^{-1}\{(e+f-2|z|)/(f-e)\} - m\pi/2]\,\mathrm{sgn}(z)\}$$

$$\times \cos(n\theta) \qquad \text{for}\quad e < |z| < f$$

$$= 0 \qquad\qquad \text{for}\quad 0 \le |z| < e,\quad f < |z| < \infty$$

$$(19)$$

where a_{mn}, b_{mn} and c_{mn} are unknown coefficients, $\mathrm{sgn}(z)$ is the signum function, and subscript b denotes the variables at $r = b$. The Fourier transformed expressions of Eqs. (17), (18) and (19) are:

$$(\bar{u}_{r1b}* - \bar{u}_{r2b}*) = \sum_{n=0}^{\infty}\{\sum_{m=1}^{\infty} a_{mn} \frac{1}{|\xi|}\sin[(e+f)|\xi|/2 - m\pi/2] \times J_m[(f-e)|\xi|/2]\}\cos(n\theta)$$

$$(\bar{u}_{\theta 1b}* - \bar{u}_{\theta 2b}*) = \sum_{n=0}^{\infty}\{\sum_{m=1}^{\infty} b_{mn} \frac{1}{|\xi|}\sin[(e+f)|\xi|/2 - m\pi/2] \times J_m[(f-e)|\xi|/2]\}\sin(n\theta)$$

$$(\bar{u}_{z1b}* - \bar{u}_{z2b}*) = -i\sum_{n=0}^{\infty}\{\sum_{m=1}^{\infty} c_{mn} \frac{1}{|\xi|}\cos[(e+f)|\xi|/2 - m\pi/2] \times J_m[(f-e)|\xi|/2]\}$$

$$\times \mathrm{sgn}(\xi)\cos(n\theta)$$

$$(20)$$

where $J_m(\xi)$ is the Bessel function. Using a method described in Ref. [2], the unknowns $A_n^{(1)}(\xi)$, $B_n^{(1)}(\xi)$ and $C_n^{(1)}(\xi)$ can be represented in terms of the coefficients a_{mn}, b_{mn} and c_{mn}. Consequently, the stress and displacement fields can both be expressed in terms of these coefficients. For example, $\tau_{rr1b}*$, $\tau_{r\theta 1b}*$ and $\tau_{rz1b}*$ can be expressed as:

$$\tau_{rr1b}* = \{\sum_{m=1}^{\infty} a_{mn} \times 1/\pi \times \int_0^{\infty} Q_1^n(\xi)/\xi \times \sin[(e+f)\xi/2 - m\pi/2]$$

$$\times J_m[(f-e)\xi/2]\cos(\xi z)d\xi\} \times \cos(n\theta)$$

$$+ \{\sum_{m=1}^{\infty} b_{mn} \times 1/\pi \times \int_0^{\infty} Q_2^n(\xi)/\xi \times \sin[(e+f)\xi/2 - m\pi/2]$$

$$\times J_m[(f-e)\xi/2]\cos(\xi z)d\xi\} \times \cos(n\theta)$$

$$+ \{\sum_{m=1}^{\infty} c_{mn} \times (-1)/\pi \times \int_0^{\infty} Q_3^n(\xi)/\xi \times \cos[(e+f)\xi/2 - m\pi/2]$$

$$\times J_m[(f-e)\xi/2]\cos(\xi z)d\xi\} \times \cos(n\theta)$$

$$\tau_{r\theta 1b}* = \{\sum_{m=1}^{\infty} a_{mn} \times 1/\pi \times \int_0^{\infty} Q_4^n(\xi)/\xi \times \sin[(e+f)\xi/2 - m\pi/2]$$

$$\times J_m[(f-e)\xi/2]\cos(\xi z)d\xi\} \times \sin(n\theta)$$

$$+ \{ \sum_{m=1}^{\infty} b_{mn} \times 1 / \pi \times \int_0^{\infty} Q_5^n(\xi) / \xi \times \sin[(e+f)\xi/2 - m\pi/2]$$

$$\times J_m[(f-e)\xi/2]\cos(\xi z)d\xi\} \times \sin(n\theta)$$

$$+ \{ \sum_{m=1}^{\infty} c_{mn} \times (-1)/\pi \times \int_0^{\infty} Q_6^n(\xi) / \xi \times \cos[(e+f)\xi/2 - m\pi/2]$$

$$\times J_m[(f-e)\xi/2]\cos(\xi z)d\xi\} \times \sin(n\theta)$$

$$\tau_{rz1b}* = \{ \sum_{m=1}^{\infty} a_{mn} \times 1/\pi \times \int_0^{\infty} Q_7^n(\xi) / \xi \times \sin[(e+f)\xi/2 - m\pi/2]$$

$$\times J_m[(f-e)\xi/2]\sin(\xi z)d\xi\} \times \cos(n\theta)$$

$$+ \{ \sum_{m=1}^{\infty} b_{mn} \times 1/\pi \times \int_0^{\infty} Q_8^n(\xi) / \xi \times \sin[(e+f)\xi/2 - m\pi/2]$$

$$\times J_m[(f-e)\xi/2]\sin(\xi z)d\xi\} \times \cos(n\theta)$$

$$+ \{ \sum_{m=1}^{\infty} c_{mn} \times (-1)/\pi \times \int_0^{\infty} Q_9^n(\xi) / \xi \times \cos[(e+f)\xi/2 - m\pi/2]$$

$$\times J_m[(f-e)\xi/2]\sin(\xi z)d\xi\} \times \cos(n\theta)$$

$$(21)$$

where the known functions $Q_1^n(\xi)$, $Q_2^n(\xi)$, $\cdots$, $Q_9^n(\xi)$ have the same expressions given in Ref. [2].

Finally, the remaining boundary condition (5) can be reduced to the following equation in the Laplace transform domain:

$$\sum_{m=1}^{\infty} \sum_{n=0}^{\infty} a_{mn} P_{mn}(x, z) + \sum_{m=1}^{\infty} \sum_{n=0}^{\infty} b_{mn} Q_{mn}(x, z) + \sum_{m=1}^{\infty} \sum_{n=0}^{\infty} c_{mn} R_{mn}(x, z) = -w_0(x, z)$$

$$\sum_{m=1}^{\infty} \sum_{n=0}^{\infty} a_{mn} S_{mn}(x, z) + \sum_{m=1}^{\infty} \sum_{n=0}^{\infty} b_{mn} U_{mn}(x, z) + \sum_{m=1}^{\infty} \sum_{n=0}^{\infty} c_{mn} V_{mn}(x, z) = -x_0(x, z)$$

$$\sum_{m=1}^{\infty} \sum_{n=0}^{\infty} a_{mn} W_{mn}(x, z) + \sum_{m=1}^{\infty} \sum_{n=0}^{\infty} b_{mn} X_{mn}(x, z) + \sum_{m=1}^{\infty} \sum_{n=0}^{\infty} c_{mn} Y_{mn}(x, z) = -y_0(x, z)$$

$$\text{for} \quad -b \leq x \leq b, \quad e \leq z \leq f$$

$$(22)$$

where

$$P_{nm}(x, z) = 1/(2\pi) \times \cos(n\theta) \times [\int_0^{\infty} [Q_1^n(\xi) / \xi - Q_1^{nL}] J_m(\varepsilon_1 \xi)$$

$$\times \{\cos(m\pi/2)[\sin(\varepsilon_3 \xi) + \sin(\varepsilon_2 \xi)]$$

$$- \sin(m\pi/2)[\cos(\varepsilon_2 \xi) + \cos(\varepsilon_3 \xi)]\} d\xi$$

$$- Q_1^{nL} \times \frac{\sin\{m\pi/2 - m\sin^{-1}(\varepsilon_3/\varepsilon_1)\}}{\sqrt{\varepsilon_1^2 - \varepsilon_3^2}} + Q_1^{nL} \times \frac{\varepsilon_1^m}{\sqrt{\varepsilon_2^2 - \varepsilon_1^2} \times \{\varepsilon_2 + \sqrt{\varepsilon_2^2 - \varepsilon_1^2}\}^m}]$$

$$Q_{nm}(x, z) = 1/(2\pi) \times \cos(n\theta) \times [\int_0^\infty [Q_2^n(\xi)/\xi] \, J_m(\varepsilon_1 \xi)$$
$$\times \{\cos(m\pi/2)[\sin(\varepsilon_3 \xi) + \sin(\varepsilon_2 \xi)]$$
$$- \sin(m\pi/2)[\cos(\varepsilon_2 \xi) + \cos(\varepsilon_3 \xi)]\} \, d\xi \quad]$$

$$R_{nm}(x, z) = -1/(2\pi) \times \cos(n\theta) \times [\int_0^\infty [Q_3^n(\xi)/\xi] \, J_m(\varepsilon_1 \xi)$$
$$\times \{\cos(m\pi/2)[\cos(\varepsilon_3 \xi) + \cos(\varepsilon_2 \xi)]$$
$$+ \sin(m\pi/2)[\sin(\varepsilon_2 \xi) + \sin(\varepsilon_3 \xi)]\} \, d\xi \quad]$$

$$S_{nm}(x, z) = 1/(2\pi) \times \sin(n\theta) \times [\int_0^\infty [Q_4^n(\xi)/\xi] \, J_m(\varepsilon_1 \xi)$$
$$\times \{\cos(m\pi/2)[\sin(\varepsilon_3 \xi) + \sin(\varepsilon_2 \xi)]$$
$$- \sin(m\pi/2)[\cos(\varepsilon_2 \xi) + \cos(\varepsilon_3 \xi)]\} \, d\xi \quad]$$

$$U_{nm}(x, z) = 1/(2\pi) \times \sin(n\theta) \times [\int_0^\infty [Q_5^n(\xi)/\xi - Q_5^{nL}] \, J_m(\varepsilon_1 \xi)$$
$$\times \{\cos(m\pi/2)[\sin(\varepsilon_3 \xi) + \sin(\varepsilon_2 \xi)]$$
$$- \sin(m\pi/2)[\cos(\varepsilon_3 \xi) + \cos(\varepsilon_2 \xi)]\} \, d\xi$$
$$- Q_5^{nL} \times \frac{\sin\{m\pi/2 - m\sin^{-1}(\varepsilon_3/\varepsilon_1)\}}{\sqrt{\varepsilon_1^2 - \varepsilon_3^2}} + Q_5^{nL} \times \frac{\varepsilon_1^m}{\sqrt{\varepsilon_2^2 - \varepsilon_1^2} \times \{\varepsilon_2 + \sqrt{\varepsilon_2^2 - \varepsilon_1^2}\}^m}]$$

$$V_{nm}(x, z) = -1/(2\pi) \times \sin(n\theta) \times [\int_0^\infty [Q_6^n(\xi)/\xi] \, J_m(\varepsilon_1 \xi)$$
$$\times \{\cos(m\pi/2)[\cos(\varepsilon_3 \xi) + \cos(\varepsilon_2 \xi)]$$
$$+ \sin(m\pi/2)[\sin(\varepsilon_2 \xi) + \sin(\varepsilon_3 \xi)]\} \, d\xi \quad]$$

$$W_{nm}(x, z) = 1/(2\pi) \times \cos(n\theta) \times [\int_0^\infty [Q_7^n(\xi)/\xi] \, J_m(\varepsilon_1 \xi)$$
$$\times \{\cos(m\pi/2)[\cos(\varepsilon_3 \xi) - \cos(\varepsilon_2 \xi)]$$
$$- \sin(m\pi/2)[\sin(\varepsilon_2 \xi) - \sin(\varepsilon_3 \xi)]\} \, d\xi \,]$$

$$X_{nm}(x, z) = 1/(2\pi) \times \cos(n\theta) \times [\int_0^\infty [Q_8^n(\xi)/\xi] \, J_m(\varepsilon_1 \xi)$$
$$\times \{\cos(m\pi/2)[\cos(\varepsilon_3 \xi) - \cos(\varepsilon_2 \xi)]$$
$$- \sin(m\pi/2)[\sin(\varepsilon_2 \xi) - \sin(\varepsilon_3 \xi)]\} \, d\xi \quad]$$

$$Y_{nm}(x, z) = -1/(2\pi) \times \cos(n\theta) \times [\int_0^\infty [Q_9^n(\xi)/\xi - Q_9^{nL}] \, J_m(\varepsilon_1 \xi)$$
$$\times \{\cos(m\pi/2)[\sin(\varepsilon_2 \xi) - \sin(\varepsilon_3 \xi)]$$
$$+ \sin(m\pi/2)[\cos(\varepsilon_3 \xi) - \cos(\varepsilon_2 \xi)]\} \, d\xi$$
$$+ Q_9^{nL} \times \frac{\sin\{m\pi/2 - m\sin^{-1}(\varepsilon_3/\varepsilon_1)\}}{\sqrt{\varepsilon_1^2 - \varepsilon_3^2}} + Q_9^{nL} \times \frac{\varepsilon_1^m}{\sqrt{\varepsilon_2^2 - \varepsilon_1^2} \times \{\varepsilon_2 + \sqrt{\varepsilon_2^2 - \varepsilon_1^2}\}^m}]$$

$$(23)$$

$$w_0(x, y) = p \ \exp[(x-b)s/c_L] \times \cos^2(\theta)/s$$

$$x_0(x, y) = -p/2 \times \exp[(x-b)s/c_L] \times \sin(2\theta)/s$$

$$y_0(x, y) = 0 . \tag{24}$$

In Eq. (23), ε_1, ε_2 and ε_3 are shown by the expressions:

$$\varepsilon_1 = (f-e)/2, \ \ \varepsilon_2 = (e+f+2z)/2, \ \ \varepsilon_3 = (e+f-2z)/2 . \tag{25}$$

The known functions $Q_1^{nL}, Q_5^{nL}, Q_9^{nL}$ in Eq. (23) have the same expressions given in Ref. [2].

The variable θ in Eqs. (23) and (24) is given by:

$$\theta = \cos^{-1}(x/b) . \tag{26}$$

Now, Eq. (22) can be solved for the unknown coefficients a_{mn}, b_{mn} and c_{mn} by means of the Schmidt method [2, 4].

5 Stress Intensity Factors

The stresses $\tau_{rr1b}{}^*$, $\tau_{r\theta1b}{}^*$ and $\tau_{rz1b}{}^*$ can be expressed by Eq. (21). If the integrands in Eq. (21) are slightly modified and the following relation is used,

$$\int_0^\infty J_n(a\xi) \, [\cos(\xi z), \, \sin(\xi z)] \, d\xi$$

$$= \{-a^n (z^2 - a^2)^{-1/2} [z + (z^2 - a^2)^{-1/2}]^{-n} \sin(n\pi/2),$$

$$a^n (z^2 - a^2)^{-1/2} [z + (z^2 - a^2)^{-1/2}]^{-n} \cos(n\pi/2)\} \qquad for \quad a < z \tag{27}$$

the stress intensity factors can be determined in the Laplace domain as follows:

$$K_{I e}{}^* = [2\pi(e-z)]^{1/2} \tau_{rr1b}{}^*\big|_{z\to e-} = \sum_{n=0}^\infty \sum_{m=1}^\infty a_{mn} \, Q_1^{nL} \cos(n\theta)/\sqrt{2\pi(f-e)}$$

$$K_{III e}{}^* = [2\pi(e-z)]^{1/2} \tau_{r\theta1b}{}^*\big|_{z\to e-} = \sum_{n=0}^\infty \sum_{m=1}^\infty b_{mn} \, Q_5^{nL} \sin(n\theta)/\sqrt{2\pi(f-e)}$$

$$K_{II e}{}^* = [2\pi(e-z)]^{1/2} \tau_{rz1b}{}^*\big|_{z\to e-} = \sum_{n=0}^\infty \sum_{m=1}^\infty c_{mn} \, Q_9^{nL} \cos(n\theta)/\sqrt{2\pi(f-e)}$$

$$\tag{28}$$

$$K_{I f}{}^* = [2\pi(z-f)]^{1/2} \tau_{rr1b}{}^*\big|_{z\to f+} = \sum_{n=0}^\infty \sum_{m=1}^\infty a_{mn} \, Q_1^{nL} (-1)^{m+1} \cos(n\theta)/\sqrt{2\pi(f-e)}$$

$$K_{III f}{}^* = [2\pi(z-f)]^{1/2} \tau_{r\theta1b}{}^*\big|_{z\to f+} = \sum_{n=0}^\infty \sum_{m=1}^\infty b_{mn} \, Q_5^{nL} (-1)^{m+1} \sin(n\theta)/\sqrt{2\pi(f-e)}$$

$$K_{II f}{}^* = [2\pi(z-f)]^{1/2} \tau_{rz1b}{}^*\big|_{z\to f+} = \sum_{n=0}^\infty \sum_{m=1}^\infty c_{mn} \, Q_9^{nL} (-1)^{m+1} \cos(n\theta)/\sqrt{2\pi(f-e)}$$

$$\tag{29}$$

The inverse Laplace transformations of the stress intensity factors are performed by the numerical method described by Miller and Guy [3].

The relation between $g^*(s)$ and $g(t)$ is expressed as:

$$\lim_{s \to 0}[s\,g^*(s)] = \lim_{t \to \infty} g(t). \tag{30}$$

The static results of the stress intensity factors in physical space can be obtained by the use of Eq. (30).

6 Numerical Examples and Results

The stress intensity factors are calculated for a Poisson's ratio $\nu = 0.3$ using quadruple precision. The crack length is denoted by $(f - e)$, and is fixed at $2b$. The Schmidt method is applied such that the infinite series in Eq. (22) are truncated by summing from $m = 1$ to 11 and from $n = 0$ to 7. The values of the left-hand side of Eq. (22) are shown in Tables 1, 2 and 3 for $(sb/c_T) = 1.4$, $e/b = 0.1$ and $f/b = 2.1$. The corresponding values of the right-hand side of Eq. (22) are in parentheses in these tables. From this data, it is evident that the Schmidt method yields satisfactory results.

Table 1
Values of

$$\sum_{m=1}^{11} \sum_{n=0}^{7} [a_{mn} P_{mn}(x/b, z/b) + b_{mn} Q_{mn}(x/b, z/b) + c_{mn} R_{mn}(x/b, z/b)]/[p/(sb/c_T)]$$

for $(sb/c_T) = 1.4$ and $e/b = 0.1$, $f/b = 2.1$. {Values of $-w_0(x/b, z/b)$ $/(sb/c_T)$ are in parentheses.}

	$x/b = $ -0.999990	0.0	0.99999
$z/b = 0.100010$	-0.1599065 (-0.1599094)	-0.0000120 (0.0)	-0.7139420 (-0.7142661)
1.10000	-0.1599341 (-0.1599094)	0.0000045 (0.0)	-0.7142271 (-0.7142661)
2.09990	-0.1599560 (-0.1599094)	0.0000519 (0.0)	-0.7145377 (-0.7142661)

Table 2
Values of

$$\sum_{m=1}^{11} \sum_{n=0}^{7} [a_{mn} S_{mn}(x/b, z/b) + b_{mn} U_{mn}(x/b, z/b) + c_{mn} V_{mn}(x/b, z/b)]/[p/(sb/c_T)]$$

for $(sb/c_T) = 1.4$ and $e/b = 0.1$, $e/b = 2.1$. {Values of $-x_0(x/b, z/b)$ $/(sb/c_T)$ are in parentheses.}

	$x/b = -0.999990$	0.0	0.999990
$z/b = 0.100010$	-0.0007148 (-0.0007151)	-0.0000538 (0.0)	0.0031924 (0.0031943)
1.100000	-0.0007151 (-0.0007151)	-0.0000064 (0.0)	0.0031940 (0.0031943)
2.099990	-0.0007150 (-0.0007151)	0.0000062 (0.0)	0.0031939 (0.0031943)

Table 3

Values of

$$\sum_{m=1}^{11} \sum_{n=0}^{7} [a_{mn} W_{mn}(x/b,\,z/b) + b_{mn} X_{mn}(x/b,\,z/b) + c_{mn} Y_{mn}(x/b,\,z/b)]/[p/(sb/c_T)]$$

for $(sb/c_T) = 1.4$ and $e/b = 0.1,\ f/b = 2.1$. {Values of $-y_0(x/b,\,z/b)/(sb/c_T)$ are in parentheses.}

	$x/b = -0.999990$	0.0	0.999990
$z/b = 0.100010$	-0.0001789 (0.0)	-0.0006812 (0.0)	0.0010880 (0.0)
1.100010	0.0000022 (0.0)	-0.0000136 (0.0)	0.0000231 (0.0)
2.099990	-0.0001837 (0.0)	0.0006479 (0.0)	-0.0010225 (0.0)

      The stress intensity factors are inverted numerically in physical space; these factors are affected by the values of the parameters δ, β, and N in Miller and Guy's method [3]. However, if the value in physical space varies slowly with time, the numerical Laplace inversion can be performed readily, as described in Ref. [1]. The present Laplace inversion is such a case. The numerical Laplace inversions were performed by setting $\beta = 0.0$, $\delta = 0.2$ and $N = 13$.

      The dynamic stress intensity factors $K_{I\,e}$ at $\theta = (0^0,\ 180^0)$, $K_{III\,e}$ at $\theta = 90^0$ and $K_{II\,e}$ at $\theta = (0^0,\ 180^0)$ were plotted against $c_T\,t/b$ in Fig. 5 for $e/b = 0.1$. The values of $K_{I\,f}$ at $\theta = (0^0,\ 180^0)$, $K_{III\,f}$ at $\theta = 90^0$ and $K_{II\,f}$ at $\theta = (0^0,\ 180^0)$ are plotted for $e/b = 0.1$ in Fig. 6.
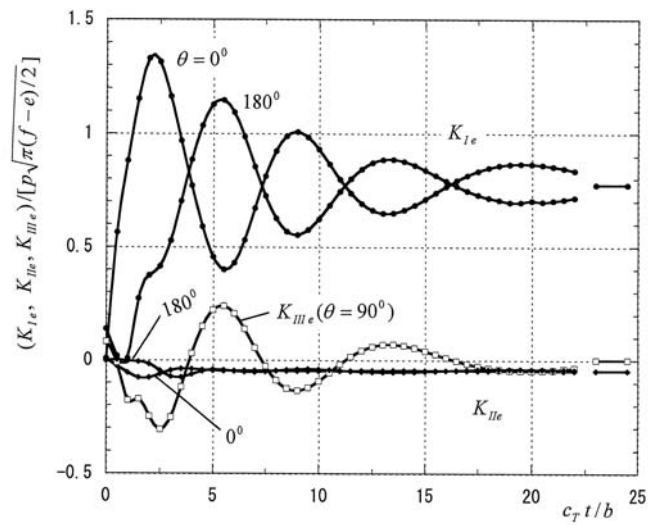
Figure 5 The dynamic stress intensity factors K_{Ie} at $\theta = (0^0, \ 180^0)$, K_{IIIe} at $\theta = 90^0$ and K_{IIe} at $\theta = (0^0, \ 180^0)$ for $e/b = 0.1$.

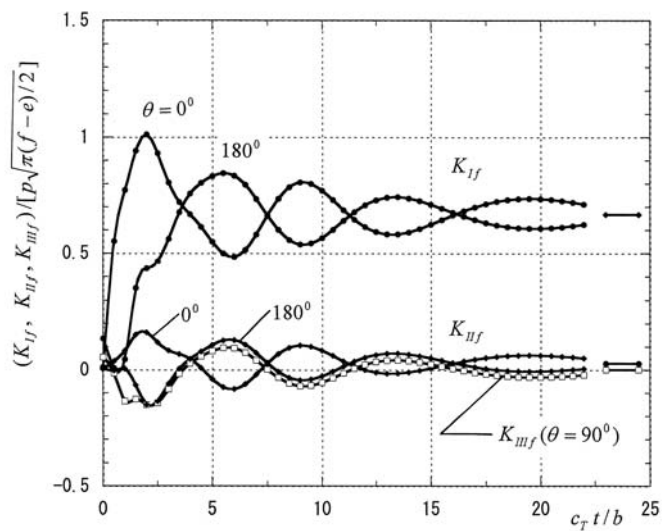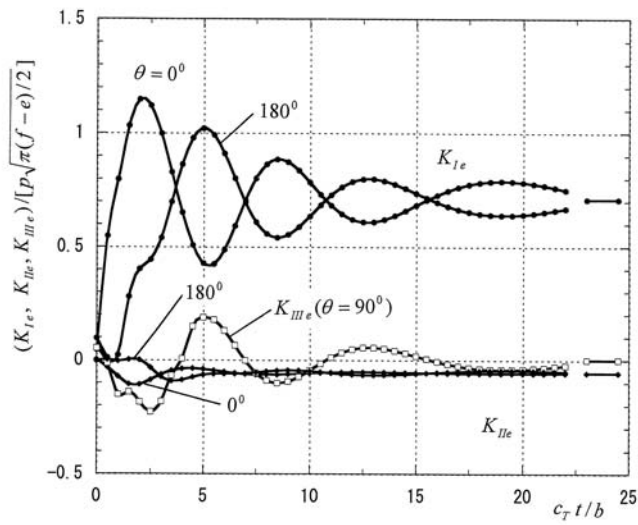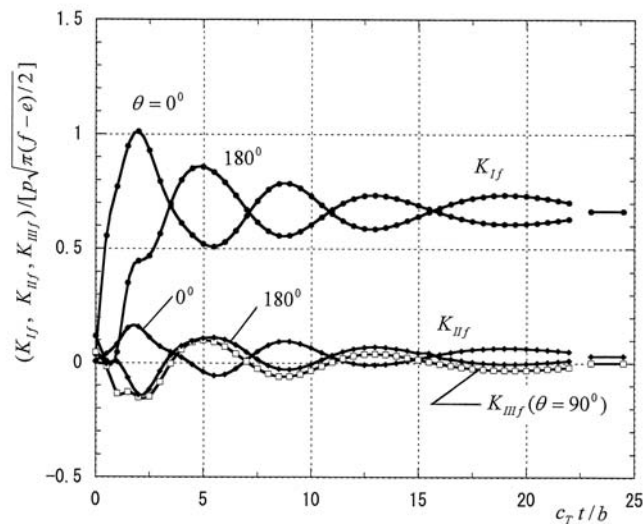Figure 6 The dynamic stress intensity factors K_{If} at $\theta = (0^0, \ 180^0)$, K_{IIIf} at $\theta = 90^0$ and K_{IIf} at $\theta = (0^0, \ 180^0)$ for $e/b = 0.1$.

Figure 7 The dynamic stress intensity factors K_{Ie} at $\theta = (0^0,\quad 180^0)$, K_{IIIe} at $\theta = 90^0$ and K_{IIe} at $\theta = (0^0,\quad 180^0)$ for $e/b = 0.2$.

Figure 8 The dynamic stress intensity factors K_{If} at $\theta = (0^0,\quad 180^0)$, K_{IIIf} at $\theta = 90^0$ and K_{IIf} at $\theta = (0^0,\quad 180^0)$ for $e/b = 0.2$.
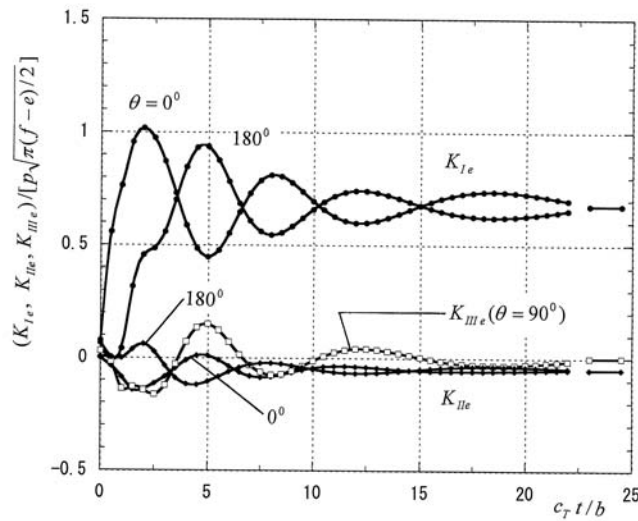
Figure 9 The dynamic stress intensity factors K_{Ie} at $\theta = (0^0, \quad 180^0)$, K_{IIIe} at $\theta = 90^0$ and K_{IIe} at $\theta = (0^0, \quad 180^0)$ for $e/b = 0.5$.
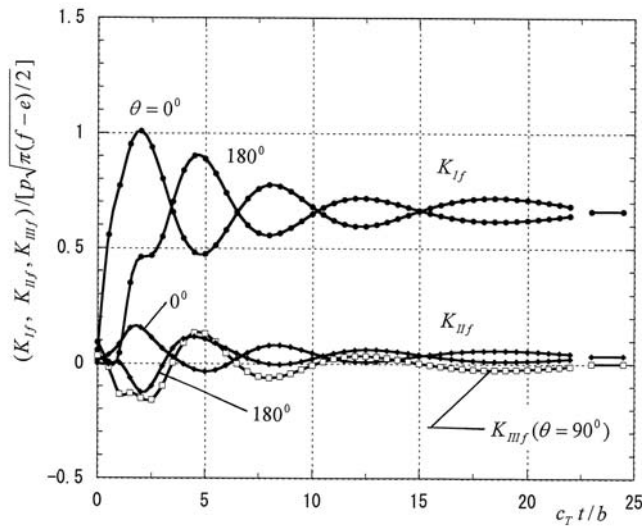

Figure 10 The dynamic stress intensity factors K_{If} at $\theta = (0^0, \quad 180^0)$, K_{IIIf} at $\theta = 90^0$ and K_{IIf} at $\theta = (0^0, \quad 180^0)$ for $e/b = 0.5$.

The corresponding values of the dynamic stress intensity factors are plotted in Figs. 7 and 8 for $e/b = 0.2$, and in Figs. 9 and 10 for $e/b = 0.5$, respectively. The straight lines on the right hand side of Figs. 5 through 10 indicate the corresponding static values that are obtained by the use of Eq. (30).

7 Discussion

A dynamic crack problem for two non-planar cracks such as two shell-shaped cracks may only be solved using a numerical method. However, in order to ascertain whether the numerical values are reliable or not, it is necessary to check the numerical results against results obtained analytically. If a numerical method is applied to solve a dynamic problem for two cylindrical cracks in an elastic material, the results can be compared with those provided in this study. If both sets of results are coincident with each other, the practicality of the numerical method for solving the stress intensity factors for two non-planar cracks is demonstrated. The numerical results presented in this study are useful for this reason, despite the fact that the crack geometry of two co-axial cylinders is unlikely to occur in practice.

8 Conclusions

The following may be concluded from the numerical calculations:

(i) The largest value of the stress intensity factors is the peak value of K_{Ie}
    at $\theta = 0^0$ and it appears near $c_T t / b = 2.0$. A consequent design consideration
    is that the fracture toughness of the material exceeds this peak stress intensity
    factor by a sufficient margin.

(ii) The values of the stress intensity factors K_{If} at $\theta = (0^0, \ 180^0)$, K_{IIIf}
    at $\theta = 90^0$ and K_{IIf} at $\theta = (0^0, \ 180^0)$ are not significantly affected by
    the distance $2e$ between the inner edges of the two cylindrical cracks. The
    values of the dynamic stress intensity factors are similar to those for a single
    cylindrical crack [2].

(iii) The maximum peak value of K_{Ie} at $\theta = 0^0$ for $e/b = 0.1$ is 1.3 times
    larger than the corresponding value for a single cylindrical crack. It is
    difficult to estimate whether this ratio would exceed 1.3 as the e/b ratio
    decreases.

References

[1] S. Itou, Dynamic stress concentration around a circular hole in an infinite elastic strip, ASME J. Appl. Mech., 50 (1983), 57-62.

[2] S. Itou, Dynamic stress intensity factors around a cylindrical crack in an infinite elastic medium subject to impact load, Int. J. Solids and Structures, 44 (2007), 7340-7356.

[3] M. Miller and T. Guy, Numerical inversion of the Laplace transform by use of Jacobi polynomials, SIAM J. Numer. Anal., 3 (1966), 624-635.

[4] P. M. Morse and H. Feshbach, Methods of Theoretical Physics Vol. 1, McGraw-Hill, New York, 1958.

[5] R. Parnes, Response of an infinite elastic medium to traveling loads in a cylindrical bore, ASME J. Appl. Mech., 36 (1969), 51-58.